

## Substructure based structural damage detection with limited input and output measurements

Y. Lei<sup>\*1,2</sup>, C. Liu<sup>1</sup>, Y.Q. Jiang<sup>1</sup> and Y.K. Mao<sup>1</sup>

<sup>1</sup>Department of Civil Engineering, Xiamen University, Xiamen 361005, China

<sup>2</sup>State Key Laboratory for Disaster Reduction in Civil Engineering, Tongji University, Shanghai 200092, China

(Received July 17, 2012, Revised March 2, 2013, Accepted March 27, 2013)

**Abstract.** It is highly desirable to explore efficient algorithms for detecting structural damage of large size structural systems with limited input and output measurements. In this paper, a new structural damage detection algorithm based on substructure approach is proposed for large size structural systems with limited input and output measurements. Inter-connection effect between adjacent substructures is treated as ‘additional unknown inputs’ to substructures. Extended state vector of each substructure and its unknown excitations are estimated by sequential extended Kalman estimator and least-squares estimation, respectively. It is shown that the ‘additional unknown inputs’ can be estimated by the algorithm without the measurements on the substructure interface DOFs, which is superior to previous substructural identification approaches. Also, structural parameters and unknown excitation are estimated in a sequential manner, which simplifies the identification problem compared with other existing work. Structural damage can be detected from the degradation of the identified substructural element stiffness values. The performances of the proposed algorithm are demonstrated by several numerical examples and a lab experiment. Measurement noise effect is considered. Both the simulation results and experimental data validate that the proposed algorithm is viable for structural damage detection of large size structural systems with limited input and output measurements.

**Keywords:** structural identification; structural damage detection; substructure approach; extended Kalman estimator; least-squares estimation; unknown inputs

### 1. Introduction

Detecting structural damage of large size structural systems is an important but still challenging task because damage is an intrinsically local phenomenon. Various structural damage detection techniques have been proposed. Among them, approaches based on structural identification (SI) have received great attention (Chang 2009, 2011, Meier *et al.* 2009, Wu *et al.* 2003, Ghanem and Shinozuka 1995). Structural damage can be identified based on tracking the changes of identified values of structural parameters, e.g., the degradation of element stiffness parameters. However, as an inverse problem, damage detection by the conventional SI approach is challenging for large size structural systems with a large number of unknown parameters due to ill-condition and computation convergence problems. In addition, as the size of a structural system increases, its

---

\*Corresponding author, Professor, E-mail: [ylei@xmu.edu.cn](mailto:ylei@xmu.edu.cn)

computational efforts increase tremendously (Koh *et al.* 2005). Consequently, substructural identification approaches have been proposed, in which a large size structure is decomposed into smaller size substructures with fewer DOFs and unknown parameters, e.g., Koh *et al.* developed several traditional and nontraditional substructural identification methods with numerical and experimental studies (Koh *et al.* 2005, Trinh and Koh 2011, Tee 2009). Xu (2005) proposed a substructural damage Diagnosis methodology with Neural Networks. Hou *et al.* (2011) described a method for substructure isolation. Huang and Yang (2008) proposed a sequential nonlinear least-square method and substructure approach to detect structural damage in the substructure. Law and Yong (2011) also proposed a substructure method for structural condition assessment. However, most of the previous substructural identification approaches require that measurements of all responses at the substructure interface DOFs are available. In practice, it is often impossible to measure all responses at the interface DOFs between substructures, e.g., it's very difficult to measure the rotational DOFs at the substructure interfaces for beam/frame structures. Although Koh *et al.* (2003) investigated substructural Identification method in frequency domain without interface measurement, the method is applicable for measured harmonic force of excitation. Some other researchers have also tried to overcome this problem (Weng *et al.* 2011, Law *et al.* 2011).

For large size civil structures, it is usually impossible to measure all external excitations to structures. Identification of structural parameters without all excitation information has been explored by some researchers (Ling and Haldar 2004, Kathuda *et al.* 2005, Chen and Li 2004, Yang *et al.* 2007, Xu *et al.* 2012). In these approaches, information about structural displacement and velocity response signals are either assumed to be available or they are obtained through integration of measured acceleration responses. In practice, dynamic responses are often measured by accelerometers. Errors are incurred in obtaining velocity and displacement signals by integration (Ling and Haldar 2004, Kathuda *et al.* 2005, Chen and Li 2004). Hence, direct use of acceleration response signals is preferred over velocity and displacement signals. Some other iterative or weighted iterative least-squares estimation approaches have been proposed to simultaneously identify structural parameters and unknown inputs (Ling and Haldar 2004, Xu *et al.* 2012).

On the other hand, it is often impossible to deploy so many sensors to measure all responses of large size structural systems. Thus, it is highly desirable to explore efficient algorithms which can detect structural damage utilizing only a limited number of measured responses of structures (Glaser *et al.* 2007). Extended Kalman filter (EKF) approach has been studied and shown to be useful too for data fusion and structural identification with limited response outputs (Hoshiya and Saito 1984, Lei *et al.* 2007), but it often leads to the problems of ill-condition and computation convergence for the identification of large-size structural systems (Lee and Yun 2008). Moreover, the traditional EKF approaches require that all excitation inputs are measured. Recently, Yang *et al.* (Yang *et al.* 2007) proposed an extended Kalman filter with unknown excitation inputs, referred to as EKF-UI, for the identification of structural parameters as well as the unmeasured excitation inputs. However, when EKF-UI is used for large-size structural systems, but it still requires the deployment of sensors to measure all responses at the substructure interface DOFs for the identification of substructures (Huang and Yang 2008).

In this paper, a time-domain algorithm based on substructure approach is proposed for detecting structural damage of large size structural systems with limited excitation input and response output measurements. Inter-connection effect between adjacent substructures is treated as 'additional unknown inputs' to substructures. Extended state vector of each substructure and its unknown excitations are estimated by sequential extended Kalman estimator and least-squares

estimation (Lei *et al.* 2007). Instead of the application of the extended Kalman filter, the Kalman estimator approach, which has been widely used in structural control, is used herein. Due to the superiority of proposed algorithm, i.e., recursive solution for the extended state vector of each substructure is initially obtained followed by the estimation of its unknown excitation values, the ‘additional unknown inputs’ to substructure can be estimated without the measurements at the substructure interface DOFs. Also, structural parameters and unknown excitation are estimated in a sequential manner, which simplifies the identification problem compared with other existing work. Structural damage is detected from the changes of substructural parameters at the element level, such as the degradation of element stiffness parameters. The effectiveness of the proposed algorithm is demonstrated by several numerical examples including the benchmark building established by the American Society of Civil Engineers (ASCE) for structural health monitoring (Bernal and Beck 2004, Johnson *et al.* 2004), a plane truss and a continuous beam in finite element models and a lab experiment on a multi-story building model.

## 2. The proposed algorithm

Based on the finite-element model, the equation of motion of a linear structural system under unknown external excitation can be written as

$$M\ddot{x}(t) + C\dot{x}(t) + Kx(t) = Bf(t) + B^u f^u(t) \tag{1}$$

in which  $x(t)$ ,  $\dot{x}(t)$  and  $\ddot{x}(t)$  are vectors of displacement, velocity and acceleration response, respectively;  $M$ ,  $C$  and  $K$  are the mass, damping and stiffness matrices, respectively;  $f(t)$  is a measured external excitation vector;  $f^u(t)$  is an unmeasured external excitation vector; and  $B$  and  $B^u$  are the influence matrices associated with  $f(t)$  and  $f^u(t)$ , respectively. Usually, the mass of a structural system can be estimated with accuracy based on its geometry and material information.

Identification of a large-size structural system is difficult as it involves a large number of DOFs and unknown parameters. Identification by the conventional system identification approaches, including the extended Kalman filter approach, often leads to the problems of ill-condition and computation convergence. In addition, as the size of a structure increases, its computational efforts increase tremendously (Koh *et al.* 1991, Trinh and Koh 2011). To reduce computational burdens and the difficulty in obtaining reasonably accurate results of damage detection, it is reasonable to apply substructure approach for large-size structural systems (Koh *et al.* 1991, Trinh and Koh 2011, Tee *et al.* 2009, Xu 2005, Hou *et al.* 2011, Huang and Yang 2008, Law and Yong 2011, Koh and Shankar 2003, Weng *et al.* 2011, Law *et al.* 2011).

### 2.1 Substructure approach

A large-size linear structural system is decomposed into a set of smaller sizes substructures based on its finite-element model. As shown in Fig. 1, the equation of motion of the concerned substructure- $r$  can be extracted from Eq. (1) to yield as

$$[M_{rr} \ M_{rs}] \begin{bmatrix} \ddot{x}_r(t) \\ \ddot{x}_s(t) \end{bmatrix} + [C_{rr} \ C_{rs}] \begin{bmatrix} \dot{x}_r(t) \\ \dot{x}_s(t) \end{bmatrix} + [K_{rr} \ K_{rs}] \begin{bmatrix} x_r(t) \\ x_s(t) \end{bmatrix} = B_r f_r(t) + B_r^u f_r^u(t) \tag{2}$$

where subscript ‘ $r$ ’ denotes the DOFs of the concerned substructure- $r$  and subscript ‘ $s$ ’ denotes the interface DOFs. Then, Eq. (2) can be re-arranged as

$$\mathbf{M}_{rr}\ddot{\mathbf{x}}_r(t) + \mathbf{C}_{rr}\dot{\mathbf{x}}_r(t) + \mathbf{K}_{rr}\mathbf{x}_r(t) = \mathbf{B}_r\mathbf{f}_r(t) + \mathbf{B}_r^u\mathbf{f}_r^u(t) - \mathbf{M}_{rs}\ddot{\mathbf{x}}_s(t) - \mathbf{C}_{rs}\dot{\mathbf{x}}_s(t) - \mathbf{K}_{rs}\mathbf{x}_s(t) \quad (3)$$

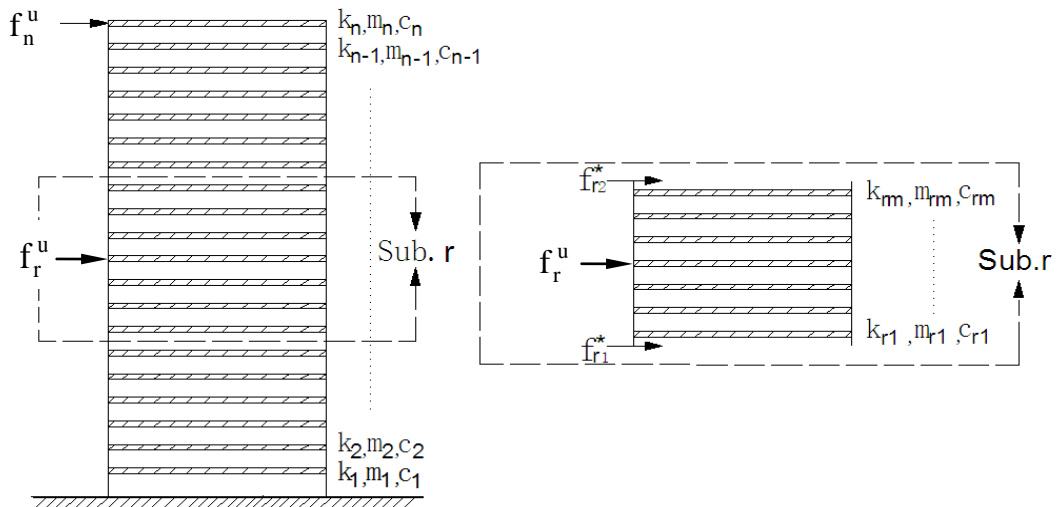
By treating the interface forces as ‘additional unknown inputs’ to the concerned substructure, Eq. (3) can be expressed as follows

$$\mathbf{M}_{rr}\ddot{\mathbf{x}}_r(t) + \mathbf{C}_{rr}\dot{\mathbf{x}}_r(t) + \mathbf{K}_{rr}\mathbf{x}_r(t) = \mathbf{B}_r\mathbf{f}_r(t) + \mathbf{B}_r^u\mathbf{f}_r^u(t) + \mathbf{B}_r^*\mathbf{f}_r^*(t) \quad (4)$$

where  $\mathbf{f}_r^*(t)$  is the ‘additional unknown input’ vector,  $\mathbf{B}_r^*$  is the influence matrix associated with the ‘additional unknown inputs’  $\mathbf{f}_r^*(t)$ , and

$$\mathbf{B}_r^*\mathbf{f}_r^*(t) = -\mathbf{M}_{rs}\ddot{\mathbf{x}}_s(t) - \mathbf{C}_{rs}\dot{\mathbf{x}}_s(t) - \mathbf{K}_{rs}\mathbf{x}_s(t) \quad (5)$$

Therefore, as shown by Fig. 1(b), unknown excitations to the concerned substructure include the unmeasured external excitation  $\mathbf{f}_r^u(t)$  and the ‘additional unknown inputs’  $\mathbf{f}_r^*(t)$  due to substructure inter-connection effect. Thus, it is required to identify these unknown excitations.



(a) A Sketch of substructures      (b) Substructure with interface forces and external excitation

Fig. 1 Substructure approach

### 2.2 Estimation of the extended state vector of substructure by extended Kalman estimator

The extended state vector of a concerned substructure is defined as

$$\mathbf{X}_r = [\mathbf{X}_{r1}^T, \mathbf{X}_{r2}^T, \boldsymbol{\theta}_r^T]^T; \mathbf{X}_{r1} = \mathbf{x}_r; \mathbf{X}_{r2} = \dot{\mathbf{x}}_r; \boldsymbol{\theta}_r^T = [\theta_{r1}, \theta_{r2}, \dots, \theta_{rm}]^T \quad (6)$$

i.e.,  $\mathbf{X}_{r1}$  is the displacement vector,  $\mathbf{X}_{r2}$  is the velocity vector, and  $\boldsymbol{\theta}_r^T$  is a vector of the  $m$ -unknown substructural parameters, such as damping and stiffness parameters. As the structural parameters are time invariant, Eq. (4) can be written in the following extended state equation for the extended state vector as follows

$$\begin{Bmatrix} \dot{\mathbf{X}}_{r1} \\ \dot{\mathbf{X}}_{r2} \\ \dot{\boldsymbol{\theta}}_r \end{Bmatrix} = \begin{Bmatrix} \mathbf{X}_{r2} \\ \mathbf{M}_{rr}^{-1} [\mathbf{B}_r \mathbf{f}_r(t) + \mathbf{B}_r^u \mathbf{f}_r^u(t) + \mathbf{B}_r^* \mathbf{f}_r^*(t) - \mathbf{C}_{rr} \mathbf{X}_{r2} - \mathbf{K}_{rr} \mathbf{X}_{r1}] \\ \mathbf{0} \end{Bmatrix} \quad (7)$$

As observed from Eq. (7), the extended state equation is a nonlinear equation of the extended state vector  $\mathbf{X}_r$ , so Eq. (7) can be rewritten in the following general nonlinear differential state equation as

$$\dot{\mathbf{X}}_r = \mathbf{g}_r(\mathbf{X}_r, \mathbf{f}_r, \mathbf{f}_r^u, \mathbf{f}_r^*) \quad (8)$$

Usually, only a limited number of accelerometers are deployed on the concerned substructures to measure its acceleration responses. Therefore, the discretized observation equation can be expressed as

$$\mathbf{y}_r[k] = \mathbf{D}_{rr} \mathbf{M}_{rr}^{-1} \{ \mathbf{B}_r \mathbf{f}_r[k] + \mathbf{B}_r^u \mathbf{f}_r^u[k] + \mathbf{B}_r^* \mathbf{f}_r^*[k] - \mathbf{C}_{rr} \mathbf{X}_{r2}[k] - \mathbf{K}_{rr} \mathbf{X}_{r1}[k] \} + \mathbf{v}_r[k] \quad (9)$$

in which  $\mathbf{y}_r[k]$  is the observation vector (measured acceleration responses) at time  $t = k \times \Delta t$  with  $\Delta t$  being the sampling time step,  $\mathbf{f}_r[k]$ ,  $\mathbf{f}_r^u[k]$ ,  $\mathbf{f}_r^*[k]$ ,  $\mathbf{X}_{r1}[k]$  and  $\mathbf{X}_{r2}[k]$  are the corresponding discretized values at time  $t = k \times \Delta t$ ,  $\mathbf{D}_{rr}$  is the matrix associated with the locations of accelerometers, and  $\mathbf{v}_r[k]$  is the measured noise vector assumed to be a Gaussian white noise vector with zero mean and a covariance matrix  $E[\mathbf{v}_{ri} \mathbf{v}_{rj}^T] = \mathbf{R}_{rij} \delta_{ij}$ , where  $\delta_{ij}$  is the Kronecker delta. As observed from Eq. (9), the observation vector is also a nonlinear function of the extended state vector. Thus, the discretized observation vector can be expressed by the following equation as

$$\mathbf{y}_r[k] = \mathbf{h}_r(\mathbf{X}_r[k], \mathbf{f}_r[k], \mathbf{f}_r^*[k]) + \mathbf{G}_r^u \mathbf{f}_r^u[k] + \mathbf{v}_r[k] \quad (10)$$

where

$$\begin{aligned} \mathbf{G}_r^u &= \mathbf{D}_{rr} \mathbf{M}_{rr}^{-1} \mathbf{B}_r^u & ; \\ \mathbf{h}_r(\mathbf{X}_r[k], \mathbf{f}_r[k], \mathbf{f}_r^*[k]) &= \mathbf{D}_{rr} \mathbf{M}_{rr}^{-1} \{ \mathbf{B}_r \mathbf{f}_r[k] + \mathbf{B}_r^* \mathbf{f}_r^*[k] - \mathbf{C}_{rr} \mathbf{X}_{r2}[k] - \mathbf{K}_{rr} \mathbf{X}_{r1}[k] \} \end{aligned}$$

Based on the approach of extended Kalman estimator (Hsieh and Chen 1999), which has been widely used in structural control, the extended state vector at time  $t = (k+1) \times \Delta t$  can be estimated with the observation of  $(\mathbf{y}_r[1], \mathbf{y}_r[2], \dots, \mathbf{y}_r[k])$  as follows

$$\hat{\mathbf{X}}_r[k+1|k] = \tilde{\mathbf{X}}_r[k+1|k] + \mathbf{K}_r[k] \left\{ \mathbf{y}_r[k] - \mathbf{h}_r(\hat{\mathbf{X}}_r[k|k-1], \mathbf{f}_r[k], \mathbf{f}_r^*[k|k-1]) - \mathbf{G}_r^u \hat{\mathbf{f}}_r^u[k|k] \right\} \quad (11)$$

in which

$$\tilde{\mathbf{X}}_r[k+1|k] = \hat{\mathbf{X}}_r[k|k-1] + \int_{t[k]}^{t[k+1]} \mathbf{g}_r(\mathbf{X}_r, \mathbf{f}_r, \mathbf{f}_r^u, \mathbf{f}_r^*) dt \quad (12)$$

$\hat{\mathbf{X}}_r[k+1|k]$  and  $\hat{\mathbf{f}}^u[k|k]$  are the estimation of  $\mathbf{X}[k+1]$  and  $\mathbf{f}^u[k]$  given  $(\mathbf{y}_r[1], \mathbf{y}_r[2], \dots, \mathbf{y}_r[k])$ , respectively and  $\mathbf{K}_r[k]$  is the Kalman gain matrix given by (Hsieh and Chen 1999) as

$$\mathbf{K}_r[k] = \Phi_r[k] \mathbf{P}_r[k] \mathbf{H}_r^T[k] (\mathbf{H}_r[k] \mathbf{P}_r[k] \mathbf{H}_r^T[k] + \mathbf{R}_r[k])^{-1} \quad (13)$$

and

$$\Phi_r[k] = \mathbf{I}_r + \mathbf{A}_r[k] \Delta t; \mathbf{A}_r[k] = \left. \frac{\partial \mathbf{g}_r(\mathbf{X}_r, \mathbf{f}_r, \mathbf{f}_r^u, \mathbf{f}_r^*)}{\partial \mathbf{X}_r} \right|_{\mathbf{X}_r = \hat{\mathbf{X}}_r[k|k-1]; \mathbf{f}_r = \mathbf{f}_r[k]; \mathbf{f}_r^u = \hat{\mathbf{f}}_r^u[k|k]; \mathbf{f}_r^* = \hat{\mathbf{f}}_r^*[k|k-1]} \quad (14)$$

$$\mathbf{H}_r[k] = \left. \frac{\partial \mathbf{h}_r(\mathbf{X}_r, \mathbf{f}_r, \mathbf{f}_r^*)}{\partial \mathbf{X}} \right|_{\mathbf{X}_r = \hat{\mathbf{X}}_r[k|k-1]; \mathbf{f}_r = \mathbf{f}_r[k]; \mathbf{f}_r^u = \hat{\mathbf{f}}_r^u[k|k]; \mathbf{f}_r^* = \hat{\mathbf{f}}_r^*[k|k-1]} \quad (15)$$

$\mathbf{I}_r$  is an identity matrix,  $\mathbf{P}_r[k]$  is the error covariance matrix of  $\hat{\mathbf{X}}_r[k|k-1]$ , and  $\mathbf{P}_r[k+1]$ , the error covariance matrix of  $\hat{\mathbf{X}}_r[k+1|k]$ , is recursively given by

$$\mathbf{P}_r[k+1] = \Phi_r[k] \mathbf{P}_r[k] \Phi_r^T[k] - \mathbf{K}_r[k] \mathbf{H}_r[k] \mathbf{P}_r[k] \Phi_r^T[k] \quad (16)$$

However, since both the external excitation  $\mathbf{f}_r^u(t)$  and the ‘additional unknown inputs’  $\mathbf{f}_r^*(t)$  are unknown, it is impossible to obtain recursive solution for the extended state vector of the concerned substructure based on the classical extended Kalman estimator alone.

### 2.3 Estimation of substructural interface forces

For the special case that measurements are available at all the DOFs of the substructure interface, the matrix  $\mathbf{G}_r^*$  in Eq. (10) is a non-zero matrix. Given the observation of  $(\mathbf{y}_r[1], \mathbf{y}_r[2], \dots, \mathbf{y}_r[k+1])$ , the ‘additional unknown disturbances’  $\mathbf{f}_r^*$  can be estimated directly from Eq. (10) based on least square estimation. Therefore, for this special case, identification of substructure works independently.

For the general case that measurements (sensors) are not available at all of the DOFs at the substructure interface, the extended state vector of each substructure at time  $t = (k+1) \times \Delta t$  can be estimated by the extended Kalman estimator given the observation signal  $(\mathbf{y}_r[1], \mathbf{y}_r[2], \dots, \mathbf{y}_r[k])$  as shown by Eq. (11). After the estimation of the extended vector of each substructure, the ‘additional unknown inputs’  $\mathbf{f}_r^*$  at time  $t = (k+1) \times \Delta t$  can be estimated subsequently based on their formulations as shown by Eq. (5), i.e.

$$\mathbf{B}_r^* \hat{\mathbf{f}}_r^*[k+1|k] = -\mathbf{M}_{rs} \hat{\mathbf{x}}_s[k+1|k] - \hat{\mathbf{C}}_{rs}[k+1|k] \hat{\mathbf{x}}_s[k+1|k] - \hat{\mathbf{K}}_{rs}[k+1|k] \hat{\mathbf{x}}_s[k+1|k] \quad (17)$$

where  $\hat{x}_s[k+1|k]$  and  $\hat{\dot{x}}_s[k+1|k]$  are the estimation values of corresponding state vectors at the interface DOFs,  $\hat{\ddot{x}}_s[k+1|k]$  can be estimated by the Newmark- $\beta$  method with the estimation values of  $\hat{x}_s[k+1|k]$  and  $\hat{\dot{x}}_s[k+1|k]$ . It has been verified by comparing the numerical estimations of accelerations with the real values in the numerical examples in Section 3 that the numerical errors in the estimations of accelerations are small which have limited influence on the estimations of the ‘additional unknown inputs’  $f_r^*[k+1|k]$  to the substructure.

Therefore, due to the superiority of the extended Kalman estimator in the proposed algorithm, the substructural interface forces which are treated as ‘additional unknown inputs’ to substructure can be estimated based on the formulation of ‘additional unknown inputs’ without all measurements on the substructure interface DOFs. However, in many other previous approaches including the EKF-UI (Yang *et al.* 2007), unknown excitations are initially estimated followed by the recursive solution for the extended state vector. Thus, it is necessary to measure all response signals at the substructure interfaces DOFs in the previous approaches. The benefits of the proposed algorithm over previous ones are obvious for the identification of large-size structural systems.

Based on the proposed algorithm, identification of substructures of a large-size structural system can be conducted concurrently with parallel computing; however, transmission between adjacent substructures about the estimated values of state vector at the interface DOFs is needed for the estimation of substructural interface forces.

### 2.4 Estimation of the unknown excitation inputs

In Eq. (10), the observation vector, such as the acceleration measurement, is a linear function of unknown external excitation  $f_r^u(t)$ . Under the conditions: i) the number of output measurements on the concerned substructure is greater than that of the unknown excitations, and ii) measurements (sensors) are available at all DOFs where the unknown external excitation  $f_r^u(t)$  acts on the substructure, i.e., matrix  $G_r^u$  in Eq. (10) is non-zero; the unknown external excitations on the substructure at time  $t=(k+1)\times\Delta t$  can be estimated from Eq. (10) by least-squares estimation as

$$\hat{f}_r^u[k+1|k+1] = [(G_r^u)^T G_r^u]^{-1} (G_r^u)^T \{y_r[k+1] - h(\hat{X}[k+1|k], f[k+1|k+1], f_r^*[k+1|k])\} \quad (18)$$

in which,  $\hat{f}_r^u[k+1|k+1]$  is the estimation of  $f_r^u[k+1]$  given the observation of  $(y_r[1], y_r[2], \dots, y_r[k+1])$ .

In summary, the main procedures of the proposed algorithm are presented as follows:

- (1) Decompose a large-size structure into a set of smaller sizes substructures and extract the equations of motion of the substructures as shown by Eq. (2)
- (2) Treat the substructure interface forces on the right side of Eq. (3) as ‘additional unknown inputs’  $f_r^*(t)$  to the substructure.
- (3) Conduct the recursive estimation of the extended state vector of each substructure  $\hat{X}_r[k+1|k]$  by the extended Kalman estimator as shown by Eqs. (11)-(16).
- (4) Estimate the recursive solution of each substructural interface forces  $f_r^*(t)$  and external excitation  $f_r^u(t)$  by Eqs. (17) and (18), respectively.

(5) Repeat the procedures (3)-(4) for the recursive estimation of the extended state vector of each substructure until the converged estimations of the substructure parameters are obtained.

Then, detect structural damage based on the degradation of element stiffness parameters in substructures.

Therefore, the proposed algorithm is based on sequential application of the extended Kalman estimator for recursive solution of extended state vector and least-squares estimation of the unknown excitation inputs, recursive solutions for the extended state vector of each substructure is initially obtained with the observation signals and unknown excitation values at a former time instant, followed by the estimation of unknown excitation values. Such straightforward derivation and analytical solutions are not available in the previous literature. Also, structural parameters and unknown excitation are estimated in a sequential manner, which simplifies the identification problem compared with other existing work.

### 3. Numerical example validations of the proposed algorithms

To demonstrate the effectiveness of the proposed algorithm for detecting structural damage of large size structural systems with limited input and output measurement, several numerical simulation examples, including the ASCE benchmark building for structural health monitoring (Bernal and Beck 2004, Johnson *et al.* 2004), a large size plane truss and a continuous beam in finite element models, are presented in this paper. The influence of measurement noise on the results of system identification and damage detection is considered by superimposition of noise process with the theoretically computed response quantities, as described in each numerical example.

In practice, damping ratios rather than damping parameters are identified. In this connection, the Rayleigh damping assumption is employed in this study and the damping matrix is assumed as

$$C = \alpha M + \beta K \quad (19)$$

where  $\alpha$  and  $\beta$  are two Rayleigh damping coefficients which depend on structural damping ratios and frequencies.

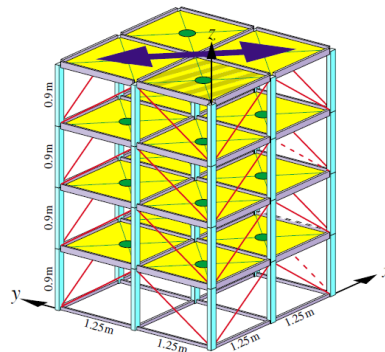
#### 3.1 The phase I ASCE benchmark structure

A benchmark building of four-story frame was established by the ASCE in order to compare the efficiencies of various system identification and damage detection techniques (Bernal and Beck 2004, Johnson *et al.* 2004). In this paper, the complex case of three dimension (3D) building + limited sensors is considered as shown in Fig. 2(a); however, limited accelerometers are deployed at the 1st and 4th floors of the benchmark building. The building is a 3D 12-DOFs shear-beam model with unknown excitation applied on the diagonal of the top floor. Since there are 16 unknown stiffness parameters as shown in Fig. 2 and the size of extend state vector of the whole building is quite large, substructural identification approach is adopted for this complex case. The benchmark building is divided into two substructures as shown in Fig. 2(b), in which substructure 1 contains the 1st and 2nd floors of the building and substructure 2 contains the 3rd and 4th floors of the building. The inter-connection effect between the two substructures is treated as the 'additional unknown inputs' to each substructure, e.g.,  $f_1^*(t)$ ,  $f_2^*(t)$  and  $f_3^*(t)$  are the

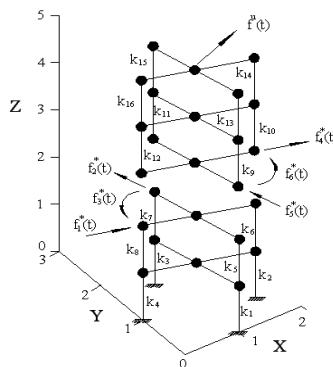
‘additional unknown inputs’ to substructure 1 while  $f_4^*(t), f_5^*(t)$  and  $f_6^*(t)$  are the ‘additional unknown inputs’ to substructure 2. As there is no sensor deployed on the 3rd floor, responses at the substructure interface DOFs are not measured. The substructural interface forcers which are treated as ‘additional unknown inputs’ to substructure are estimated based on their formations as shown by Eq. (18).

It should be noted that two adjacent substructures should have a common interface in the decomposition of a large-size structure into a set of substructures so that every stiffness parameters are included in the estimation of substructures. The interface forces between two adjacent substructures are not action-reaction and therefore are not the same.

The damping matrix is assumed to be in the Rayleigh damping form, as indicated by Eq.(19), with corresponding damping ratios equal to 1%. To consider the influence of measurement noise on the results of system identification and damage detection, the measured acceleration responses are simulated by the theoretically computed responses superimposed with the corresponding white noise with 5% noise- to- signal ratio in root mean square (RMS). Based on the proposed algorithm for the estimation of the extended state vector of the two substructures, element stiffness, Rayleigh damping coefficients, the displacement and velocity responses of the building can be identified. Structural damage is detected by tracking the degradation of identified element stiffness parameters.



(a) The Phase I ASCE benchmark building



(b) The substructure of ASCE benchmark building

Fig. 2 The ASCE Benchmark building with substructure approach

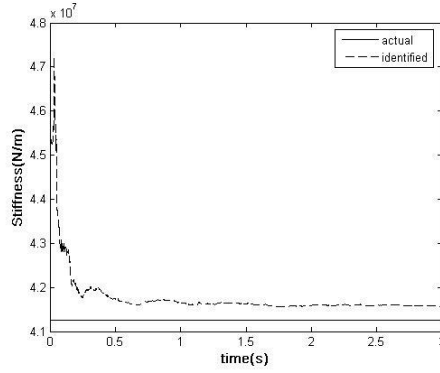
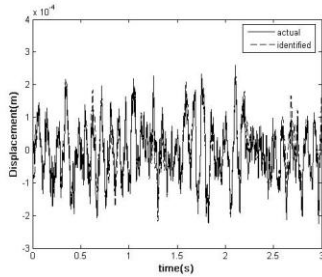
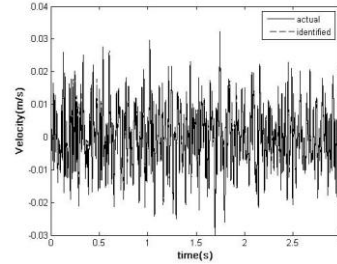


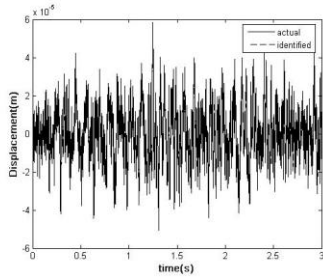
Fig. 3 Convergence of identified  $k_0$  for building with DP4



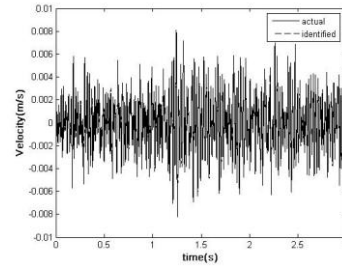
(a) Comparison of the 4th floor displacement response in X direction (DP4)



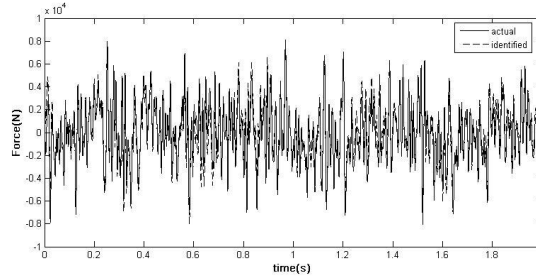
(b) Comparison of the 4th floor velocity response in X direction (DP4)



(c) Comparison of the 4th floor displacement response in rotational direction (DP4)



(d) Comparison of the 4th floor velocity response in rotational direction (DP4)



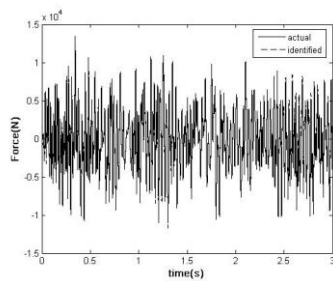
(e) Comparison of unknown external excitation for building with DP4

Fig. 4 Comparison of identified responses and excitation

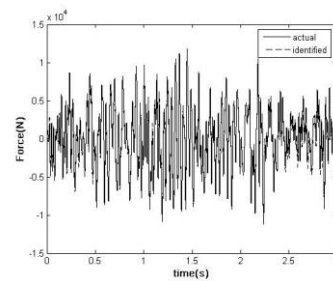
The first four damage patterns in the benchmark problem (Bernal and Beck 2004, Johnson *et al.* 2004) are studied herein, i.e., damage patterns include damage pattern 1 (DP1): all braces in the first story are removed, damage pattern 2 (DP2): all braces in both the 1st and 3rd floors are removed, damage pattern 3 (DP3): one brace is removed in the 1st story, and damage pattern 4 (DP4): one brace is removed in each of the 1st and 3rd stories.

Fig. 3 shows the convergence of the identified element stiffness values. It is noted that the identified stiffness parameter converges very fast. For clarity of comparisons, some identified displacement and velocity responses in the X and rotational directions for a segment from 0.0 to 3.0 s are presented in Figs. 4(a)–4(d) as dashed curves while the corresponding actual results are also shown as solid curves in these figures. The identified unknown excitation on the 4th floor for a segment from 0.0 to 2.0 s is also shown in Fig. 4(e) as the dashed curve with comparison to the actual white noise excitation presented as the solid curve. In Figs. 5(a)–5(d), estimation results of ‘additional unknown inputs’  $f_1^*(t)$  and  $f_2^*(t)$  to substructure one and  $f_5^*(t)$  and  $f_6^*(t)$  to substructure two are shown by dash curves with comparisons to their corresponding real values shown by solid curves. From the above comparisons, it is validated that the proposed algorithm can estimate structural responses, elements parameters, inter-connection effect between adjacent substructures and the unknown external excitation to the structure with very good accuracy.

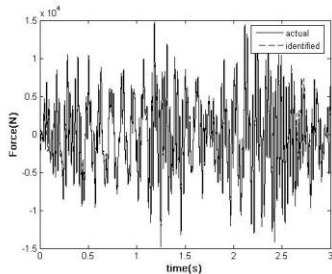
Identification results of all story stiffness for the undamaged building and the damage one with the aforementioned four damage patterns are shown in Table 1, whereas the exact story stiffness values are also shown for comparison. It is observed from the above comparisons that the proposed algorithm is capable of detecting structural damage based on the degradation of the identified values of element stiffness parameters as shown by the data in bold-face in Table 1.



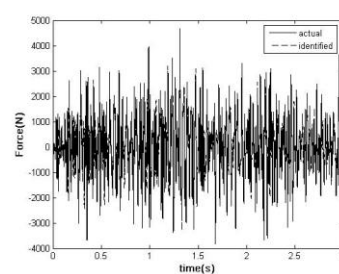
(a) Comparison of  $f_1^u$  for building with DP4



(b) Comparison of  $f_2^u$  for building with DP4



(c) Comparison of  $f_5^u$  for building with DP4



(d) Comparison of  $f_6^u$  for building with DP4

Fig. 5 Comparison of identification interface forces

Table1 Damage detection results of the ASCE benchmark building

Stiffness No.	Undamaged (Exact) [MN/m]	Undamaged (Identified) [MN/m]	DP1 (Identified) [MN/m]	DP2 (Identified) [MN/m]	DP3 (Identified) [MN/m]	DP4 (Identified) [MN/m]
$k_1$	53.31	52.33	<b>28.72</b>	<b>29.15</b>	52.96	51.74
$k_2$	33.96	32.87	<b>9.51</b>	<b>9.97</b>	<b>22.52</b>	<b>22.28</b>
$k_3$	53.31	52.81	<b>29.37</b>	<b>29.78</b>	53.26	51.74
$k_4$	33.96	33.23	<b>9.85</b>	<b>9.82</b>	33.75	32.64
$k_5$	53.31	53.61	54.41	52.35	54.75	55.12
$k_6$	33.96	34.90	34.30	32.67	35.27	32.16
$k_7$	53.31	53.57	54.77	52.67	51.67	54.82
$k_8$	33.96	34.23	33.43	33.43	33.43	33.43
$k_9$	53.31	52.97	52.86	<b>29.89</b>	54.31	<b>41.58</b>
$k_{10}$	33.96	32.96	33.58	<b>9.47</b>	34.79	34.64
$k_{11}$	53.31	53.75	55.45	<b>30.34</b>	54.66	51.01
$k_{12}$	33.96	34.69	34.59	<b>10.23</b>	35.21	34.08
$k_{13}$	53.31	52.93	54.13	52.12	52.04	52.04
$k_{14}$	33.96	34.87	33.15	32.75	34.75	34.95
$k_{15}$	53.31	53.81	52.24	54.64	52.22	54.82
$k_{16}$	33.96	33.63	34.75	34.85	32.35	34.71

### 3.2 A large size plane truss structure

As show in Fig. 6(a), identification of a large-size simply supported plane truss subject to an unmeasured external excitation is taken as another numerical example to illustrate the proposed algorithm. Assume that the truss consists of 23 bars with the same uniform cross section area  $A=8.947 \times 10^{-5} m^2$ , Young's modulus  $E=2 \times 10^7 pa$ , and the mass density  $\rho = 7850 kg/m^3$ . The length of each horizontal bar is  $2m$  while the length of each inclined bar is  $\sqrt{2} m$ . Structural global mass matrix  $M$  and stiffness matrix  $K$  can be formulated as the summation of each element mass and stiffness matrices, in which the stiffness of  $i$ -th truss element is defined as  $k_i = EA/l_i$ .

In the substructure approach for this large-size truss, the truss is divided into three small-size trusses as shown in Fig. 6(b). The inter-connection effect between adjacent two substructures is treated as the 'additional unknown inputs' to each substructure, i.e.,  $f_1^*(t), f_2^*(t)$  and  $f_3^*(t)$  are the 'additional unknown inputs' to substructure 1 from substructure 2,  $f_4^*(t), f_5^*(t), f_6^*(t)$  and  $f_7^*(t), f_8^*(t), f_9^*(t)$  are the 'additional unknown inputs' to substructure 2 from substructure 1 and 3, respectively, and  $f_{10}^*(t), f_{11}^*(t), f_{12}^*(t)$  are the 'additional unknown inputs' to substructure 3 from substructure 2. In the numerical example, it is assumed that there are no accelerometers deployed

on the nodes 4 and 8, so acceleration responses at the substructural interface DOFs are not all measured.

The external excitation is assumed to be a white noise, but it is also not measured. Again, all the measured acceleration responses are simulated by the superimposing theoretically computed responses with the corresponding stationary white noise with 5% noise-to-signal ratio in RMS. Based on the proposed algorithm, structural responses, structural parameters and the unknown excitation of each substructure can be identified with parallel computation among the three substructures.

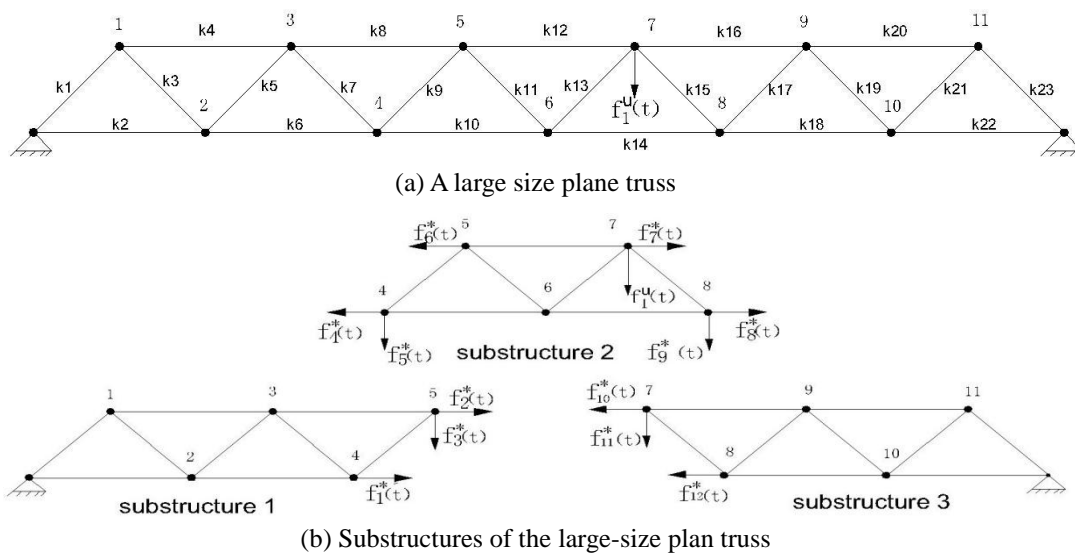
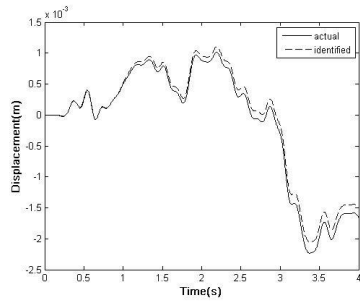


Fig. 6 A large size plane truss with substructure approach

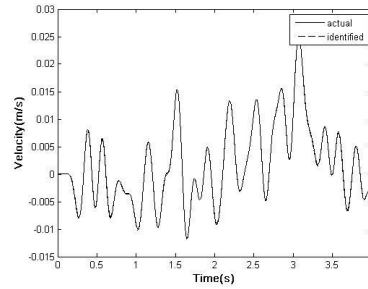
Estimated results of displacement and velocity responses in the lateral and vertical directions at node 1 are presented in Figs. 7(a) and 7(b) as dashed curves, respectively. To verify the identification results, the corresponding actual results are also shown as solid curves in these figures for comparisons. In Figs. 8(a) and 8(b), estimation results of two ‘additional unknown inputs’  $f_1^*(t)$  and  $f_9^*(t)$  are shown by dash curves with comparisons to their corresponding real values shown by solid curves. The identified unknown excitation is also shown in Fig. 8(c) as the dashed curve with comparison to the actual white noise excitation presented as the solid curve. From these comparisons, it is shown that substructural responses and inter-connection effect between adjacent substructures can be identified with good accuracies by the proposed algorithm. The identified unknown excitation also compares well with the actual one.

Supposed damage occurs in both the 2nd and 22nd bars which cause both  $k_2$  and  $k_{22}$  reduce from 894.76N/m to 626.33N/m. Based on the proposed distributed identification algorithm, the stiffness parameters of the truss in undamaged pattern and the damage pattern can be identified. Identification results of element stiffness converge very fast, but the convergence processes are not shown herein due to space limitation. Element stiffness values of all bars in the undamaged and damaged patterns are identified and shown in the 4th and 7th column of Table 2, respectively.

From the comparison of the identified results with their analytical values, it is shown that the proposed method can identify structural element stiffness parameters with good accuracy and structural damage can be detected and located from the degradation of the identified element stiffness parameters as shown by the data in bold-face in Table 2.

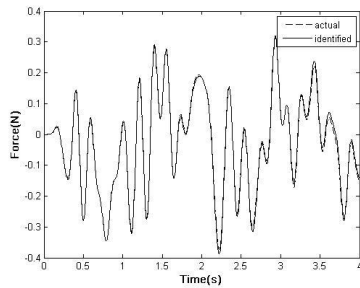


(a) Comparison of lateral displacement response of node 1

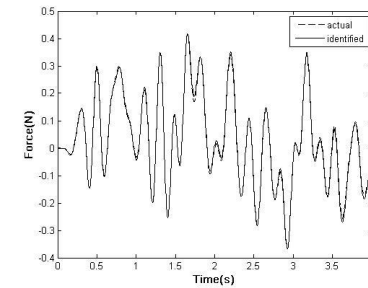


(b) Comparison of vertical velocity response of node 1

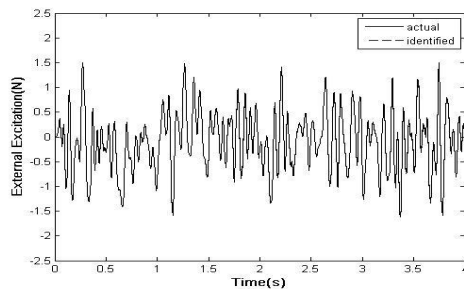
Fig. 7 Comparisons of identified responses



(a) Comparison of 'additional unknown input'  $f_1^*(t)$



(b) Comparison of 'additional unknown input'  $f_9^*(t)$



(c) Comparison of unknown external excitation

Fig. 8 Comparison of identified interface forces and unknown excitation

Table2 Damage detection results of a large-size plan truss

Sub No.	Bar No.	Bar stiffness $k_i$ (N/m)					
		Undamaged (Exact)	Undamaged (Identified)	Error (%)	Damaged (Exact)	Damaged (Identified)	Error (%)
Sub 1	1	1265.4	1251.9	-1.07	1265.4	1262.9	-0.19
	2	<b>894.8</b>	<b>897.5</b>	<b>0.31</b>	<b>626.3</b>	<b>618.8</b>	<b>-1.21</b>
	3	1265.4	1263.9	-0.11	1265.4	1266.2	0.06
	4	894.8	903.8	1.01	894.8	889.3	-0.61
	5	1265.4	1237.6	-2.19	1265.4	1218.3	-3.72
	6	894.8	891.0	-0.42	894.8	899.5	0.53
	7	1265.4	1280.3	1.18	1265.4	1290	1.95
	8	894.8	900.7	0.66	894.8	892.1	-0.30
	9	1265.4	1266.8	0.11	1265.4	1298.8	2.64
Sub 2	9	1265.4	1256.6	-0.69	1265.4	1267.6	0.18
	10	894.8	898.7	0.44	894.8	895.9	0.13
	11	1265.4	1252.8	-0.99	1265.4	1257	-0.67
	12	894.8	852.4	-4.73	894.8	887.7	-0.79
	13	1265.4	1278.2	1.02	1265.4	1270.2	0.38
	14	894.8	878.9	-1.77	894.8	886.9	-0.88
	15	1265.4	1268.6	0.26	1265.4	1278.2	1.01
Sub 3	15	1265.4	1278.1	1.00	1265.4	1270.5	0.41
	16	894.8	884.0	-1.20	894.8	887.1	-0.86
	17	1265.4	1262.5	-0.23	1265.4	1276.9	0.91
	18	894.8	884.9	-1.11	894.8	888	-0.76
	19	1265.4	1275.0	0.76	1265.4	1263	-0.19
	20	894.8	895.1	0.04	894.8	900.9	-0.69
	21	1265.4	1275.8	0.82	1265.4	1256.4	-0.71
	22	<b>894.8</b>	<b>898.0</b>	<b>0.37</b>	<b>626.3</b>	<b>624.3</b>	<b>-0.32</b>
	23	1265.4	1260.8	-0.36	1265.4	1265.1	0.02

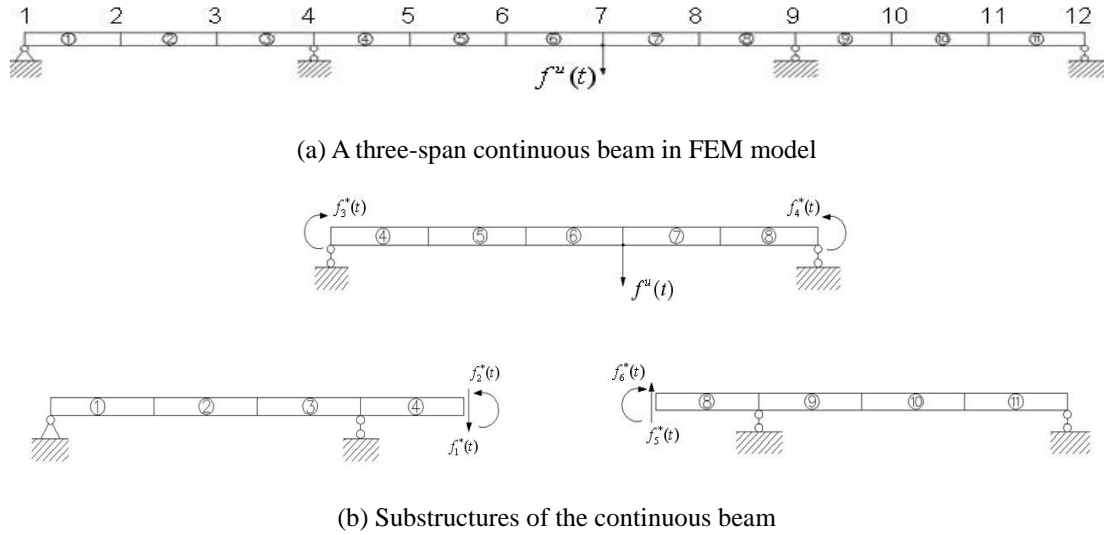


Fig. 9 A three-span continuous beam with substructure approach

### 3.3 A three-span continuous beam in finite element model

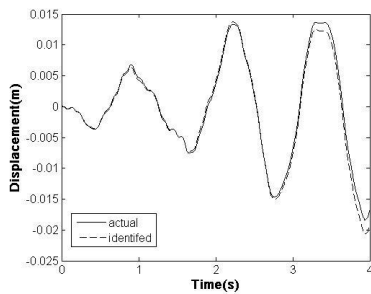
A simply supported three-span continuous beam with uniform cross section, as shown in Fig. 10(a), is considered as the final numerical example to illustrate the proposed algorithm. A finite element model of the beam is also shown in Fig. 9(a), in which the beam is divided into 11 elements with equal length. Each element has two nodes with two DOFs in the vertical and rotational directions, respectively, except nodes 1 and 12 have only rotational DOF due to the constraints at the two ends. In this example, the beam is assumed to be in bending deformation without axial forces. The beam is subjected to an unknown (unmeasured) external excitation in the vertical direction at node 7.

In the numerical example, it is assumed that cross section area  $A=0.1m^2$  and length of the beam element  $l=1.5$  m, mass density  $\rho=7850$   $kg/m^3$ , Young's modulus  $E=2\times 10^8$  pa.  $k=EI/l$ , which is defined as the equivalent stiffness of the element with  $I$  being the moment inertia, is selected as  $222.22\times 10^3$   $kN\cdot m$ . Global mass matrix of the whole continuous beam is assumed to a contracted one while the global stiffness matrix of the whole beam can be obtained based on assembling all the element stiffness matrices. Structural damping ratios are assumed as  $\xi_1 = \xi_2 = 0.03$ .

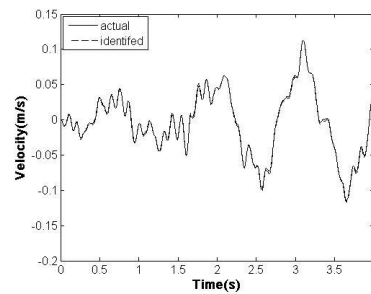
Since the size of the extended state vector of the whole beam is quite large, substructural approach is adopted in which the continuous beam is divided into three small-size substructure as shown in Fig. 9(b). The inter-connection effect between adjacent two substructures is treated as the 'additional unknown inputs' to each substructure, i.e.,  $f_1^*(t)$  and  $f_2^*(t)$  are the 'additional unknown inputs' to substructure 1 from substructure 2,  $f_3^*(t)$  and  $f_4^*(t)$  are the 'additional unknown inputs' to substructure 2 from substructure 1 and 3, respectively, and  $f_5^*(t)$  and  $f_6^*(t)$  are the 'additional unknown inputs' to substructure 3 from substructure 2.

In practice, it's still a problem to have appropriate instruments for measuring dynamic responses of rotational angles. Therefore, it's not reasonable to have the measurements of

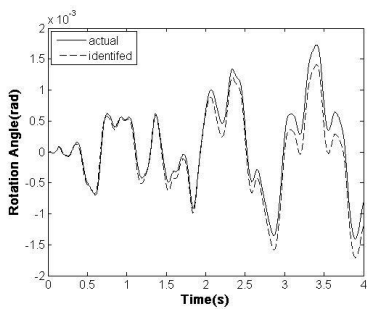
acceleration responses of the rotational DOFs, acceleration responses in the vertical directions at node 2, 3, 5, 6, 7, 8, 10, 11 are measured. Therefore, only limited acceleration responses are measured and the responses at the substructural interface DOFs are not all available. Again, all the measured acceleration responses are simulated by the superimposing theoretically computed responses with the corresponding stationary white noise with 5% noise-to-signal ratio in RMS.



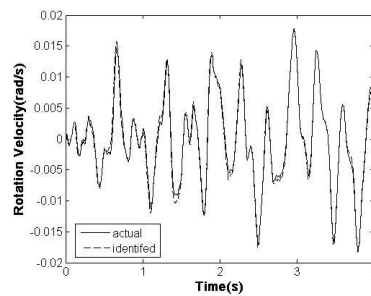
(a) Comparison of vertical displacement response at node 6



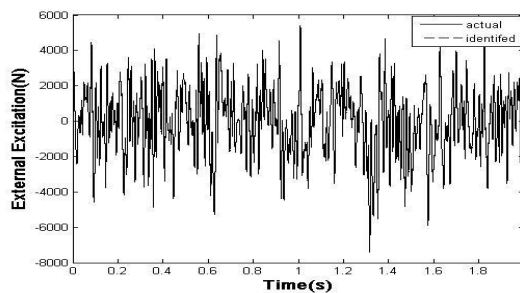
(b) Comparison of vertical velocity response at node 6



(c) Comparison of rotational response at node 3



(d) Comparison of velocity of rotational response at node 3



(e) Comparison of unknown external excitation

Fig. 10 Comparisons of identified responses and excitation

Based on the proposed algorithm, estimated results of the vertical responses at node 6 are presented in Figs. 10(a) and 11(b) as dashed curves, respectively. Also, estimation results for the rotational response at node 3 are shown by dashed curves in Figs. 10(c) and 11(d), respectively. To

verify the identification results, the corresponding actual results are also shown by solid curves in these figures for comparisons. The identified unknown excitation is also compared with the actual white noise excitation in Fig. 10(e), in which the identified unknown excitation is shown as the dashed curve with comparison to the actual white noise excitation presented as the solid curve. Estimation results of ‘additional unknown inputs’ compares well with their corresponding real values, but these comparisons are not shown herein due to space limitation. From these comparisons, it is shown that substructural responses and inter-connection effect between adjacent substructures can be identified with good accuracies by the proposed algorithm. The identified unknown excitation also compares well with the actual one.

Identification results of equivalent stiffness of elements converge very fast, but the convergence processes are not shown herein due to space limitation. The converged results and the results of all equivalent stiffness of elements for undamaged beam are shown in the third column in Table 3 with comparisons to the exact values. It is observed from these comparison results that the proposed algorithm can accurately estimate structural elements stiffness parameters.

Supposed structural damage occur in element 1, 6, 10, the proposed algorithm is utilized to identify all equivalent element stiffness of the damaged beam. The identification results are shown in the 6th column in Table 3. From the comparisons in Table 3, it is demonstrated that the proposed algorithm is capable of detecting and localizing structural damage from the degradation of the identified equivalent element stiffness parameters as shown by the data in bold-face in Table 3.

Table3 Damage detection results of a three-span continuous beam

Element No.	Stiffness $k_i$ (kN·m)					
	Undamaged (Exact)	Undamaged (Identified)	Error (%)	Damaged (Exact)	Damaged (Identified)	Error (%)
1	222.22	223.98	0.79	<b>177.78</b>	<b>180.88</b>	1.74
2	222.22	222.54	0.14	222.22	215.01	-3.25
3	222.22	227.02	2.16	222.22	224.36	0.96
4	222.22	212.08	-4.56	222.22	219.92	-1.04
5	222.22	220.86	-0.61	222.22	222.02	-0.09
6	222.22	226.98	2.14	<b>177.78</b>	<b>185.53</b>	4.36
7	222.22	223.91	0.76	222.22	224.52	1.03
8	222.22	219.51	-1.22	222.22	216.2	-2.71
9	222.22	215.94	-2.83	222.22	213.92	-3.74
10	222.22	220.28	-0.87	<b>177.78</b>	<b>185.92</b>	4.58
11	222.22	225.49	1.47	222.22	217.9	-1.94

#### 4. Experimental validation of the proposed algorithms

An eight-story frame in the lab shown in Fig. 11(a) is used for experimental validation of the proposed algorithm. Since the building floor is much stiffer compared with the slender columns made of thin steel sheets, a theoretical lumped mass shear building is modeled for the lab frame. Mass of each floor can be estimated, so mass matrix of the building is known. The building is excited by a magnetic shake, which induces an unmeasured excitation to the building at the 3rd

story level. Six light PCB accelerometers are installed on the 2nd, 3rd, 4th, 6th, 7th and 8th floors to measure the one-dimension acceleration responses of at the corresponding floor levels (see Fig. 11(a)).

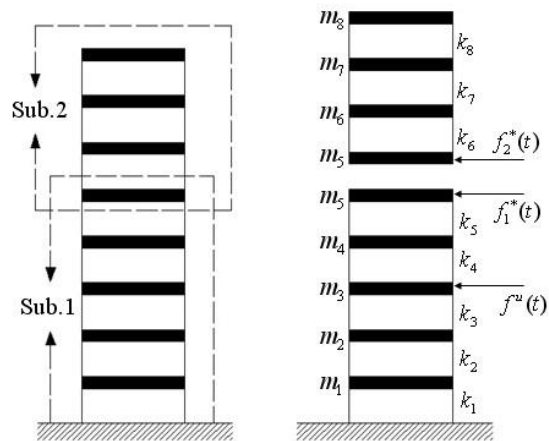
Although the lab building is not large in size, it is used as a prilitary and illustrative example for the verfiation of the proposed substructural approach, in which the building is divided into two substructures with floors 1-5 being the 1st substructure and floors 5-8 being the second one as shown as shown in Fig. 11(b). The inter-connection effect between the two substructures is treated as the ‘additional unknown inputs’ to each substructure shown in Fig. 11(b), i.e.,  $f_1^*(t)$  is the ‘additional unknown inputs’ to substructure 1 from substructure 2,  $f_2^*(t)$  is the ‘additional unknown inputs’ to substructure 2 from substructure 1. Thus, substructure 1 is excited by both the unmeasured excitation  $f^u(t)$  and the ‘additional unknown inputs’  $f_1^*(t)$ . Since there is no sensor on the 5th floor, responses at the substructure interface DOFs are not measured.

Based on the proposed algorithm for the estimation of the extended state vector, story stiffness, Rayleigh damping coefficients, the displacement and velocity responses of each substructure can be identified. Identification results of story stiffness  $k_i$  ( $i=1,2,\dots,8$ ) converge vey fast, but the convergence processes are not shown herein due to space limitation. The identification results of story element stiffness  $k_i$  are shown in the 2nd column of Table 4.

Structural damage is simulated by replacing the original slender columns by another type of thinner steel sheets, which results in the reduction of corresponding story stiffness  $k_i$  ( $i=1, 2, \dots, 8$ ). In the experiment, structural damage is assumed to occur in the columns of the 5th story which leads to the reduction of  $k_5$ . By comparing the degradation values of the identified story stiffness parameters in the 4th column in Table 4, it can be detected that structural damage occurs at the 5th columns, which conforms to the actual structural damage. The level of structural damage can also be estimated by the degradation values of  $k_5$  as shown by the data in bold-face in Table 4.



(a) An eight-story frame in the lab



(b) An eight-story frame in the lab with substructure approach

Fig. 11 An eight-story frame in the lab with substructure approach

Table 4 Identification results of story stiffness

Storey No.	Stiffness $k_i$ (kN/m)		
	Undamaged	Damaged	Degradation (%)
1	129.91	132.26	1.82
2	128.33	131.47	2.45
3	124.75	123.02	-1.39
4	126.87	122.74	-3.26
<b>5</b>	<b>136.13</b>	<b>107.21</b>	<b>-21.25</b>
6	132.79	134.33	1.16
7	140.11	137.65	-1.76
8	133.34	134.88	1.15

## 5. Conclusions

In this paper, a new structural damage detection algorithm based on substructure approach is proposed for large size structural systems with limited input and output measurements. Inter-connection effect between adjacent substructures is considered by ‘additional unknown inputs’ to substructures. By sequential application of the extended Kalman estimator for recursive solution of extended state vector of substructure and least-squares estimation of its unknown excitation inputs, it is shown that the ‘additional unknown inputs’ can be estimated by the algorithm without the measurements of the substructure interface DOFs, which is superior to previous substructural identification methods. Such straightforward derivation and analytical solutions are not available in the previous literature. Also, structural parameters and unknown excitation are estimated in a sequential manner, which simplifies the identification problem compared with other existing work. Several numerical examples and a lab experiment validate that the proposed algorithm can detect structural damage in large size structural systems with limited input and output measurements.

Limitations of the proposed algorithms include: i) the number of output measurements is larger than that of the unknown excitations, and ii) measurements (sensors) must be available at the DOFs where the unknown external excitations act. Moreover, experimental studies of large size structures are necessary to fully assess the performances of the proposed algorithm are needed. Relevant work is being undertaken by the authors.

## Acknowledgements

The authors gratefully acknowledge the supports from the National Natural Science Foundation of China (NSFC) through the Grant No. 51178406 and the research funding SLDRCE10-MB-01 from the State Key Laboratory for Disaster Reduction in Civil Engineering at Tongji University, China.

## References

- Bernal, D. and Beck, J. (Eds). (2004), "Special section: phase I of the IASC-ASCE structural health monitoring benchmark", *J. Eng. Mech. - ASCE*, **130**(1), 1-127.
- Chang, F.K. (Ed.) (2009, 2011), *Proceedings of the 6th, 7th and the 8th International Workshops on Structural Health Monitoring*, Stanford University, Stanford, CA, CRC Press, New York.
- Chen, J and Li, J. (2004), "Simultaneous identification of structural parameters and input time history from output-only measurements", *Comput. Mech.*, **33**(5), 365-374.
- Ghanem, R.G. and Shinozuka, M. (1995), "Structural system identification I: theory", *J. Eng. Mech. - ASCE*, **121**(2), 255-264.
- Glaser, S.D., Li, H., Wang, M.L., Ou, J.P. and Lynch, J.P. (2007), "Sensor technology innovation for the advancement of structural health monitoring: a strategic program of US-China research for the next decade", *Smart Struct. Syst.*, **3**(2), 221-244.
- Hoshiya, M. and Saito, E. (1984), "Structural identification by extended Kalman filter", *J. Eng. Mech.-ASCE*, **110**(12), 1757-1771.
- Hou, J.L., Jankowski, L. and Ou, J.P. (2011), "A substructural isolation method for local structural health monitoring", *Struct. Health Monit.*, **18**, 601-618.
- Hsieh, C.S. and Chen, F.C. (1999), "Optimal Solution of the Two-Stage Kalman Estimator", *IEEE T. Automat. Contr.*, **44**(1), 194-199.
- Huang, H.W. and Yang, J.N. (2008), "Damage identification of substructure for local health monitoring", *Smart Struct. Syst.*, **4**(6), 795-807.
- Johnson, E.A., Lam, H.F., Katafygiotis, L.S. and Beck, J.L. (2004), "The phase I IASC-ASCE structural health monitoring benchmark problem using simulated data", *J. Eng. Mech. - ASCE*, **130**(1), 3-15.
- Kathuda, H., Martinez, R. and Hladar, A. (2005), "Health assessment at local level with unknown input excitation", *J. Struct. Eng.- ASCE*, **131**(6), 956-965.
- Koh, C.G., See, L.M. and Balendra, T. (1991), "Estimation of structural parameters in time domain: a substructure approach", *Earthq. Eng. Struct. D.*, **20**(8), 787-801.
- Koh, C.G. and Shankar K. (2003), "Substructural identification method without interface measurement", *J. Eng. Mech. - ASCE*, **129**(7), 769-776.
- Law, S.S. and Yong, D. (2011), "Substructure methods for structural condition assessment", *J. Sound Vib.*, **330**(5), 3606-3619.
- Law, S.S., Zhang, K. and Duan, Z.D. (2011), "Structural damage detection from coupling forces between substructures under support excitation", *Eng. Struct.*, **32**(8), 2221-2228.
- Lei, Y., Lei, J.Y. and Song, Y. (2007), "Element level structural damage detection with limited observations and with unknown inputs", *Proceedings of the SPIE's Conference on Health Monitoring of Structural and Biological Systems*, 6532, 65321X1-X9, San Diego, CA, USA.
- Lee, K.J. and Yun, C.B. (2008), "Parameter identification for nonlinear behavior of RC bridge piers using sequential modified extended Kalman filter", *Smart Struct. Syst.*, **4**(3), 319-342.
- Ling, X.L. and Haldar, A. (2004), "Element level system identification with unknown input with rayleigh damping", *J. Eng. Mech. - ASCE*, **130**(8), 877-885.
- Meier, U., Havaraneck, B. and Motavalli M. (Eds.) (2009), *Proceedings of the 4th International Conference on structural health monitoring of intelligent infrastructures*, Zurich.
- Tee, K.F., Koh, C.G. and Quek, S.T. (2009), "Numerical and experimental studies of a substructural identification strategy", *Struct. Health Monit.*, **8**(5), 397-410.
- Trinh, T.N. and Koh, C.G. (2011), "An improved substructural identification strategy for large structural systems", *Struct. Health Monit.*, Article first published online, 25 MAY 2011 DOI: 10.1002/stc.463.
- Weng, S., Xia, Y., Xu, Y.L. and Zhu, H.P. (2011), "Substructure based approach to finite element model updating", *Comput. Struct.*, **89**(9-10), 772-782.
- Wu, Z.S., Xu, B. and Harada, T. (2003), "Review on structural health monitoring for infrastructures", *J. Appl. Mech. - JSCE*, **6**, 1043-1054.

- Xu, B. (2005), "Time domain substructural post-earthquake damage diagnosis methodology with neural networks", *Lecture Note Comput. Sci.*, **3611**, 520-529,
- Xu, B., Rovekamp, J.H.R. and Dyke, S.J. (2012), "Structural parameters and dynamic loading identification from incomplete measurements: approach and validation", *Mech. Syst. Signal Pr.*, **28**, 244-257.
- Yang, J.N., Pan S. and Huang, H.W. (2007), "An adaptive extended Kalman filter for structural damage identification II: unknown inputs", *Struct. Health Monit.*, **14**(3), 497-521.

FC